A STOCHASTIC VARIATIONAL INEQUALITY APPROACH THAT MODELS MICROSWIMMERS NEAR BOUNDARIES AND SUBJECT TO CHEMOTAXIS

PROPOSAL FOR CEMRACS 2018

Team: Á. Mateos González, L. Mertz, M. Tang
Montpellier University & NYU Shanghai & Shanghai Jiaotong University

- Movement of biological microswimmers near surfaces
- Competition between boundary attraction and chemotaxis
- Stochastic variational inequalities and related partial differential equations

1. The goal of the project

Biological microswimmers in confined *in vitro* media tend to concentrate in the vicinity of surfaces [14]. There are two main approaches in modeling the underlying boundary effects, namely a fluid model that describes the interactions between microswimmers and their surrounding fluid [5] and a transport and collision model with reorientation mediated by rotational brownian motion [10]. Each of the two approaches is able to reproduce experimental data observed. However, they describe different mechanisms which occur simultaneously. The relative contribution of these two types of mechanism is not clear, but microswimmer-to-wall contact seems to play a crucial role according to recent 3D microscopy techniques [7].

Our goal of this project is to build a mathematical formalism that is able to describe contact phases by considering the approach developed in [10, 9]. Techniques based on variational inequalities are applied to give a fine description of boundary effects.

More precisely, the aims of the project are the following.

- Proposing a solid model in the framework of variational inequalities inspired in [3] to describe the boundary effects. In particular, take into account the transport, the collision and translational and rotational fluctuations due to white or coloured noise.
- Reproducing the experimental observations by numerical simulations [13, 6].
- Coupling the described motion with increasingly complex models of chemotaxis – from transport following a constant concentration gradient to Keller-Segel [12].
- Deriving the associated backward and forward Kolmogorov equations, along the lines of [4, 2, 11].

Few words on the members of the project. The team members have a strong background on basic methods, at the core of the proposal, in applied stochastic analysis and PDEs. They include: **Álvaro Mateos González** (PhD Applied Mathematics, post-doctoral fellow at Montpellier University) with expertise in asymptotic analysis, PDEs, structured and integro-differential equations, and biomathematics. **Laurent Mertz** (PhD Applied Mathematics, Visiting Assistant Professor at Shanghai New York University) with expertise in applied stochastic analysis, stochastic processes and PDEs, **Min Tang** (PhD Applied Mathematics, Professor at Shanghai Jiaotong University) with expertise in mathematical models for chemotaxis and tumor growth and numerical analysis. *Laurent Mertz (LM) and Min Tang (MT) met at the time they were PhD student and postdoc at the Laboratoire Jacques Louis Lions. LM and Álvaro Mateos González (AMG) met during the CEMRACS 2017 and discussed research collaboration projects.*

Funding. Laurent Mertz can support himself and one student using his University fund. Álvaro Mateos González expects that the Labex CEMEB, NUMEV and AGRO, which fund his postdoctoral position, may partially support his expenses.

2. Model for biological microswimmers near surfaces sujject to chemotaxis

In this section, we present the framework of stochastic variational inequalities used for the description of boundary effects (see subsection 2.1) and its extension in order to include chemotactic motion (see subsection 2.2).

2.1. **Boundary effects: a stochastic variational inequality approach.** In [10], a dynamical model for the position $\{y_t, t \geqslant 0\}$ and a single orientation angle $\{\theta_t, t \geqslant 0\}$ of a microswimmer was introduced. It describes interaction with boundaries. We interpret this type of boundary interaction in terms of a variational inequality that becomes stochastic when random fluctuations are taken into account. We believe that it is helpful to accurately model the contact phases. The sum of (a) the variation of displacement along the y-axis of the microswimmer, (b) the variation of momentum of the forces from the flow and the surrounding random fluctuations applied to the microswimmer (c) the variation of momentum of the forces from the boundary interaction is zero (inertia has been neglected), i.e. $\forall t_0 < t_1$,

$$\underbrace{y_{t_1} - y_{t_0}}_{(a):displacement} = \underbrace{-\int_{t_0}^{t_1} f(\eta_s, \theta_s, y_s)\mathrm{d}s}_{(b):flow\&fluctuations} \underbrace{-(k_{t_1} - k_{t_0})}_{(c):wall}.$$

Here $f(\eta, \theta, y)$ is a drift function depending on the random fluctuation η, the position y and the orientation θ of the microswimmer. To better understand $k(.)$, consider the special case of a unilateral constraint in the sense that the extremity at $y = 0$ of the microswimmer container would be removed to $y = -\infty$ while the other one would remain at L. Then, there is an explicit expression for k_t, that is

$$k_t = \max_{0 \leqslant s \leqslant t} \left(y_0 - \int_0^s f(\eta_r, \theta_r, y_r)\mathrm{d}r - L \right)^+, \; u^+ \triangleq \max(0, u).$$

Roughly speaking, dk_t "absorbs" the part of the flow forces that would lead the microswimmer beyond the boundary. The bilateral constraint case belongs to the class of the so-called *Skorokhod problem* (SP), see for instance [15] and references therein. Adapted to the present problem, it states that *for* $w_t \triangleq -\int_0^t f(\eta_s, \theta_s, y_s)\mathrm{d}s \in \mathcal{C}([0, \infty); \mathbb{R})$ *with* $w(0) \in [0, L]$ *there exists a unique solution* (x_t, k_t) *of the SP:*

$$y_t \in \mathcal{C}([0, \infty); [0, L]),\; k_t \in \mathcal{C}([0, \infty); \mathbb{R}),\; k_t \in BV(0, T), \forall T < \infty,\; y_t + k_t = w_t, \forall t \geqslant 0.$$

and

$$y_t = \int_0^t \mathrm{sign}(y_s)\mathrm{d}|k|_s \quad \textit{and} \quad |k|_t = \int_0^t \mathbf{1}_{\{y_s \in \{0, L\}\}}\mathrm{d}|k|_s.$$

where $|k|$ *is the total variation of* k*. The last condition means that* k_t *is increasing, decreasing, constant when* $y_t = 0$*,* $y_t < L$*,* $y_t = L$*, respectively.* Here,

$$k_t = \int_0^t \max\left(0, -f(\eta_s, \theta_s, y_s)\right) \mathbf{1}_{\{y_s = L\}}\mathrm{d}s + \int_0^t \min\left(0, -f(\eta_s, \theta_s, y_s)\right)) \mathbf{1}_{\{y_s = 0\}}\mathrm{d}s,$$

and thus $\mathrm{d}k_t = -f(\eta_t, \theta_t, y_t)\mathrm{d}t$ when $y_t = 0, y_t = L$ and $\mathrm{d}k_t = 0$ when $y_t \in \{0, L\}$. In this problem, the constraint is given by an interval (convex in $\mathbb{R}$) and thus it can be recast in terms of a variational inequality [1] as follows:

$$(\mathcal{SVI}) \qquad (\dot{y}_t - f(\eta_t, \theta_t, y_t))(\varphi - y_t) \geqslant 0, \quad \forall \varphi \in [0, L], \quad \forall \varphi \in [0, L], \quad \mathrm{d}\theta_t = g(y_t, \theta_t)\,\mathrm{d}\tilde{W}_t,$$

subject to the reset condition $\theta_t = 0$ whenever $y \in \{0, L\}$. The fluctuation η_t will be considered of two forms: white noise $\eta = \dot{W}$ and coloured noise where η satisfies a stochastic differential equation of the form $\mathrm{d}\eta_t = -v'(\eta_t)\,\mathrm{d}t + \sigma\,\mathrm{d}W_t$ and v is a confining potential. Typically, $v(\eta) = \alpha\eta^2, \alpha > 0$.

2.2. **Chemotaxis model.** We intend to couple the stochastic model above, that describes boundary interactions, with several models of chemotaxis. An underlying biological motivation is that of describing the competition between boundary attraction and chemotactic motion that tend to separate swimmers from the solid boundary. Two different types of bacteria movements can be considered: 1) bacteria move by forward moving transport with some noises in their dynamics, while their forward moving directions may exhibit some fluctuations; 2) alternating forward-moving runs and reorienting tumbles. If the flagella of bacteria rotate counterclockwise (CCW), they form a bundle and push the cell to run forward with a speed

of $10\mu m/s \sim 30\mu m/s$; if the flagella rotate clockwise (CW) they fly apart and the cell tumbles in place. Bacterium can bias its movement in response to external chemical signals, e.g. towards locations with higher concentration of chemoattractant or lower concentration of repellent, and this process is called chemotaxis. Both individual based models and continuous PDE models for chemotaxis behavior have been well studied in the last decade. Classical models include

- Stochastic simulations that takes into account the noise in space and transportation in the direction of the chemical gradient.
- The Keller-Segel equation that phenomenologically takes into account the space diffusion and advection along the direction of chemical gradient.
- Describing the run and tumble process by individual based stochastic model or kinetic descriptions.

But most of them are for unbounded domains or the boundary effects have been ignored.

3. Research Plan

Here, we describe analytical and numerical tools we will adopt for the study the aforementioned models.

3.1. **Ultra weak variational formulation formulation of the density equation.** When the noise η is coloured, an approach similar that proposed in [3] is employed. Here, It is conjectured that there exists a unique invariant probability measure ν for the triple (η, θ, y) which has a `density` m composed of three positive L^1 functions $m(\eta,\theta,y)$, $m_0(\eta,\theta)$ and $m_L(\eta,\theta)$ where

$$\int_\Omega m(\eta,\theta,y)\mathrm{d}\eta\mathrm{d}\theta\mathrm{d}y + \int_{\Omega_0} m_0(\eta,\theta)\mathrm{d}\eta\mathrm{d}\theta + \int_{\Omega_L} m_L(\eta,\theta)\mathrm{d}\eta\mathrm{d}\theta = 1$$

where $\Omega \triangleq (-\infty,\infty)\times(0,2\pi]\times(0,L)$, $\Omega_0 \triangleq (-\infty,\infty)\times(0,2\pi]\times\{0\}$, $\Omega_L \triangleq (-\infty,\infty)\times(0,2\pi]\times\{L\}$. These three functions are characterized by the following ultra-weak formulation: for all functions φ `smooth` such that

$$\begin{cases} \text{reset condition at } y=0:\ \varphi(\eta,\theta,0)=\varphi(\eta,0,0), \quad \forall(\eta,\theta)\in(-\infty,\infty)\times(0,2\pi] \\ \text{reset condition at } y=L:\ \varphi(\eta,\theta,L)=\varphi(\eta,0,L), \quad \forall(\eta,\theta)\in(-\infty,\infty)\times(0,2\pi] \\ \text{periodic condition at } \theta=\{0,2\pi\}:\ \varphi(\eta,0,y)=\varphi(\eta,2\pi,y), \quad \forall(\eta,y)\in(-\infty,\infty)\times[0,L] \end{cases}$$

and

$$\int_\Omega m(\eta,\theta,y)A\varphi(\eta,\theta,y)\mathrm{d}\eta\mathrm{d}\theta\mathrm{d}y + \int_\Omega m_0(\eta,\theta)B_0\varphi(\eta,\theta)\mathrm{d}\eta\mathrm{d}\theta + \int_\Omega m_L(\eta,\theta)B_L\varphi(\eta,\theta)\mathrm{d}\eta\mathrm{d}\theta = 0,$$

where

$$\begin{aligned} A &\triangleq \frac{g(y,\theta)^2}{2}\frac{\partial^2}{\partial\theta^2} + f(y,\theta,\eta)\frac{\partial}{\partial y} + \frac{\sigma^2}{2}\frac{\partial^2}{\partial\eta^2} - v'(\eta)\frac{\partial}{\partial\eta}, \\ B_0 &\triangleq \frac{g(y,\theta)^2}{2}\frac{\partial^2}{\partial\theta^2} + \min(0,f(y,\theta,\eta))\frac{\partial}{\partial y} + \frac{\sigma^2}{2}\frac{\partial^2}{\partial\eta^2} - v'(\eta)\frac{\partial}{\partial\eta}, \\ B_L &\triangleq \frac{g(y,\theta)^2}{2}\frac{\partial^2}{\partial\theta^2} + \max(0,f(y,\theta,\eta))\frac{\partial}{\partial y} + \frac{\sigma^2}{2}\frac{\partial^2}{\partial\eta^2} - v'(\eta)\frac{\partial}{\partial\eta}. \end{aligned}$$

A similar derivation can be done in the case including chemotaxis.

3.2. **Preliminary simulations.** We rely on [6] to discretize ($\mathcal{SVI}$). Fix $T>0, N\in\mathbb{N}$ and $\Delta t \triangleq \frac{T}{N}$. We fix $(y_0,\theta_0)\in[0,L_y]\times[0,2\pi)$ and we define in an inductive manner $\{(y_n,\theta_n)\}_{n=1}^N$ as follows:

$$\begin{cases} y_{n+1} \triangleq \mathrm{proj}_{[0,\mathrm{L_y}]}\left(\mathrm{y_n} + \mathrm{V}\sin\theta_\mathrm{n}\Delta\mathrm{t} + \eta_\mathrm{n}\right) \\ \theta_{n+1} \triangleq \begin{cases} \theta_n + \sqrt{\Delta t}G_n & \text{if } y_{n+1}\in(0,L_y) \\ 0, & \text{otherwise.} \end{cases} \end{cases} \tag{1}$$

Here $\{G_n\}_{n=1}^N$ is a sequence of i.i.d. standard gaussian variables and the function $\mathrm{proj}_{[0,\mathrm{L_y}]}$, defined on $\mathbb{R}$, is the nearest neighbor projection on the interval $[0,L_y]$. The noise η_n (independant of $\{G_n\}_{n=1}^N$) can take two different forms

- $\eta_n = \sqrt{\Delta t}\tilde{G}_n$ where $\{\tilde{G}_n\}_{n=1}^N$ is a sequence of i.i.d. standard gaussian variables,

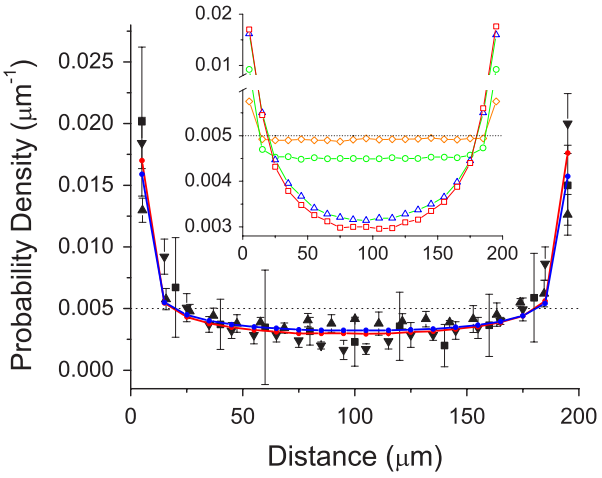

FIG. 4 (color online). Comparison between simulated density distributions at rotational diffusion constants 0.12 [blue (black)] and 0.0001 [red (gray)] rad^2/s and the measured distributions of *C. crescentus* (up triangles), *E. coli* (down triangles, Ref. [3]), and bull spermatozoa (squares, Ref. [4]). Inset compares simulated distribution at rotational diffusion constants of 10 (diamonds), 1 (circle), 0.1 (triangles), and 0.0001 (squares) rad^2/s at a swimming speed of 50 μm/s, corresponding to rod lengths of $\sim$1.3, $\sim$2.8, $\sim$6, and $\sim$60 μm, respectively. The dotted lines indicate the probability density if there is no surface accumulation.

FIGURE 1. Figure taken from [10].

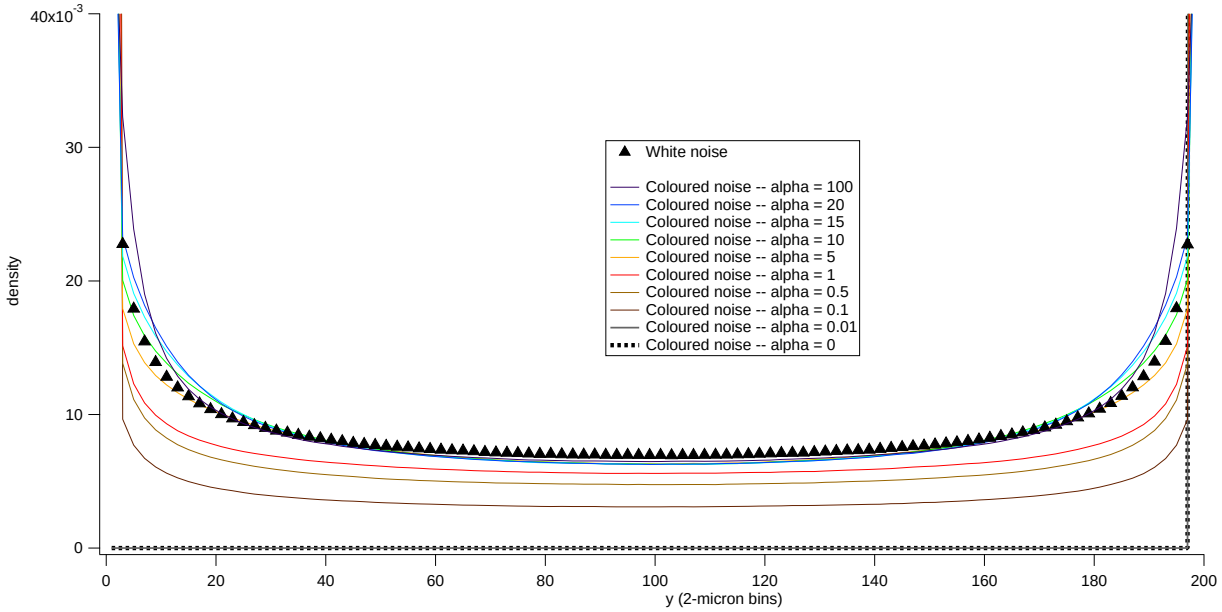

FIGURE 2. Family of probability density distribution profiles computed each by binning into 2-μm bins the successive simulated positions of microswimmer subjected to the translational noises described in the legend. The family of density profiles provides a promising ressemblance to the experimental profiles of Figure 1, while being different from the family of profiles resulting from a varying rotational diffusion coefficient also depicted in Figure 1.

- or $\{\eta_n\}_{n=1}^N$ is also defined in an inductive manner as follows

$$\eta_{n+1} \triangleq \eta_n - v'(\eta_n)\Delta t + \sigma\sqrt{\Delta t}\tilde{G}_n.$$

Such simulations produce y and θ evolution curves, a detail of which is depicted in Figure 3, that resemble those presented in [10, 9]. Binning the recorded positions for one swimmer trajectory produces density profiles that seem to approach reasonably the experimental density profiles appearing in [5, 10] – shown in Figure 1. Figure 2 depicts a family of such computed density curves for a set of parameters α of the noise involved.

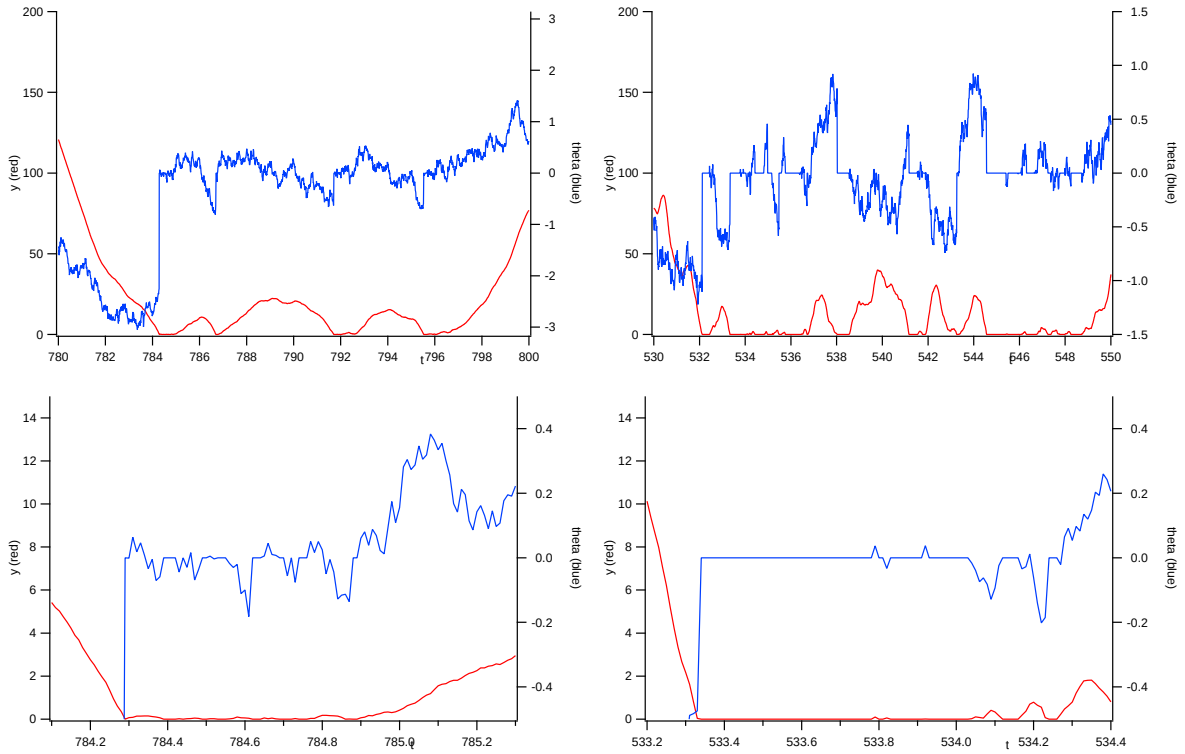

FIGURE 3. Detail of two boundary sticking phases, where the position y (red) and the angle θ (blue) of a microswimmer are depicted. The top subfigures represent time intervals of $20s$, the bottom ones represent a zoom on subintervals of the above, lasting $1.2s$. The left subfigures corresponds to a swimmer subjected to white translational noise, which, despite staying close to the boundary, often becomes unstuck from it. The right curves depict the behaviour of a swimmer subjected to coloured translational noise, with a coefficient $\alpha = 5$ corresponding to that defined in subsection 3.1. Due to the persistence of the coloured noise, the coloured noise microswimmer experiences sticking phases of positive duration. This is clearly seen on the θ curve, since the simulation enforces $\theta = 0$ when $y = 0$.

There are two main features of the simulation results that we find interesting. **The first** relates the nature of the boundary residence periods to the nature of the translational noise (see η_n above) implemented. A microswimmer subject to translational white noise seems to experience phases in which it is very close to the boundary and touches it many times, but does not stick to it, as depicted on the left subfigure of Figure 3. This was expected: indeed, in continuous time, the duration of a phase in which the microswimmer would remain at $y = 0$ (or $y = L_y$) would be 0. However, coloured noise does lead to sticking phases of a positive duration as we can see on the right subfigure of Figure 3, and as was expected. **The second** interesting feature corresponds to the qualitatively different response of translational white and coloured noise simulations to the introduction of a chemotactic transport following a constant in space and time substrate gradient. This simply corresponds to changing the way y is updated at each time step by adding $V_c\,\mathrm{dt}$. Figure 4 depicts four time-averaged density profiles corresponding to white (black) or coloured noise (red), coupled with slow (full line) or fast (dashed line) chemotactic transport. The time-averages have been taken for a single microswimmer. An ergodic property is expected in the sense that we believe that

$$\forall f,\ \lim_{T\to\infty} \int_0^T f(y_t, \theta_t, \eta_t)dt = \nu(f).$$

We observe that fast chemotactic transport induces full concentration on the upper boundary in the white noise scenario, but not in the coloured noise scenario, where a positive density exists over $[0, L_y]$. This

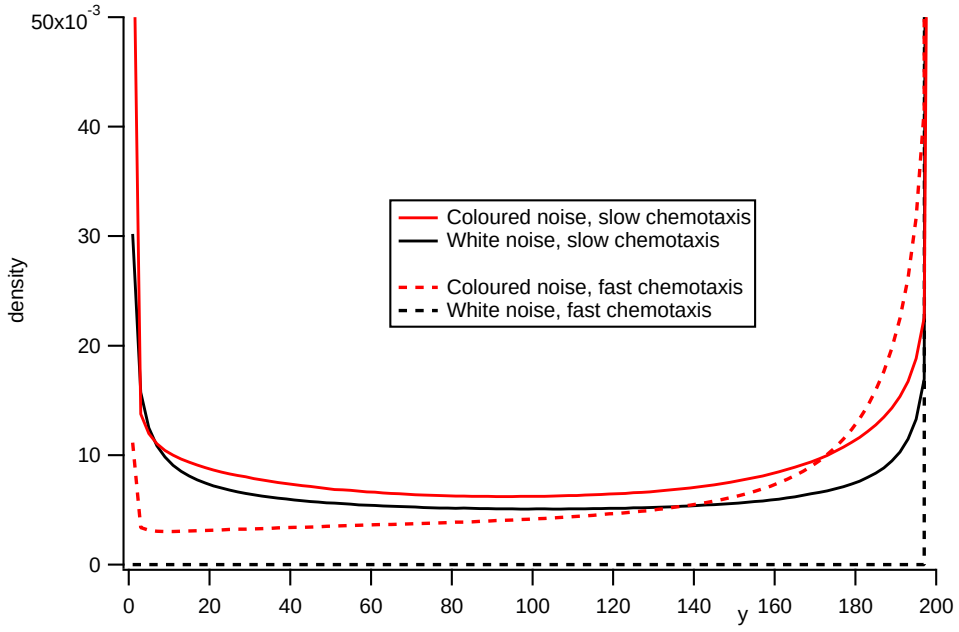

FIGURE 4. Qualitative difference of white and coloured noise effects on the concentration of a swimmer subject to chemotactic transport. The depicted curves connect dots that plot, at the centre of each of 100 bins of size $2\mu m$, the proportion of measured positions of the microswimmer that fall in that bin.

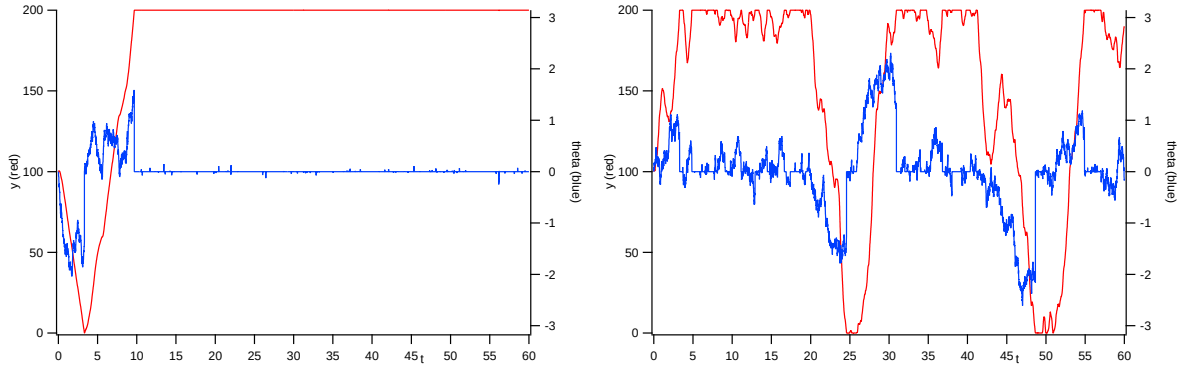

FIGURE 5. Fast chemotactic transport at $V_c = 10\mu m/s$ – swimmer velocity is still $45\mu m/s$. The left subfigure corresponds to a swimmer subjected to white translational noise, which, after a certain time, sticks to the L_y boundary and seems to be unable to swim further than a small threshold. The right curve depicts the behaviour of a swimmer subjected to coloured translational noise, with a coefficient $\alpha = 5$ corresponding to that defined in subsection 3.1. Due to the persistence of the coloured noise, the microswimmer can become unstuck from the L_y boundary and swim in the interior of the domain and visit both boundaries.

is consistent with the behaviours of the microswimmers whose coordinates are depicted in Figure 5: the coloured noise miroswimmer tends to be closer to the L_y boundary but can wander off and visit and even stick to the 0 boundary, whereas the white-noise microswimmer sticks to the L_y boundary and remains stuck. The effects that already appear in our preliminary simulations – namely, stick phase duration and competition between chemotactic transport and boundary attraction – seem promising enough and could be refined in more complex simulations and thanks to analytical studies on Kolmogorov equations related to ν.

4. Management Plan

The analytical framework we have defined above, as well as the results of our preliminary simulations, have allowed us to identifiy several interesting axes of research, which we sketch hereafter.

- Study the duration of boundary residence periods and its dependency on the parameters of the coloured translational noise.
  - Obtain statistical results from the simulations and analytical results in the framework of pdes.
- Study the competition of boundary attraction and chemotaxis in the context of both white and coloured noise.
  - Obtain statistical results.
  - Prove those are the expected statistical results.
  - Identify potential critical points thanks to simulations.
  - Prove analytically that the identified critical points are indeed critical.
- Implement more complex models of chemotaxis.
  - In the simulations, consider Keller-Segel equations with substrate consumption and production of a chemoattractant.
  - Implement a simulation of a Run and Tumble model. Compare to [8].
  - Write the kinetic stochastic system and the associated Kolmogorov equations. (difficult)
- Implement a non-punctual model of surface contact following [10, 9, 7] and compare its predictions to that of our stochastic variational equations framework.

References

[1] A. Bensoussan and J.L. Lions. Contrôle impulsionnel et inéquations quasi variationnelles. Méthodes mathématiques de l'informatique. Dunod, 1982.

[2] A. Bensoussan, L. Mertz, and S. C. P. Yam. Nonlocal boundary value problems of a stochastic variational inequality modeling an elasto-plastic oscillator excited by a filtered noise. SIAM Journal on Mathematical Analysis, 48(4):2783–2805, 2016.

[3] Alain Bensoussan and Janos Turi. Degenerate dirichlet problems related to the invariant measure of elasto-plastic oscillators. Applied Mathematics and Optimization, 58(1):1–27, Aug 2008.

[4] Alain Bensoussan and Janos Turi. On a Class of Partial Differential Equations with Nonlocal Dirichlet Boundary Conditions, pages 9–23. Springer Netherlands, Dordrecht, 2010.

[5] Allison P. Berke, Linda Turner, Howard C. Berg, and Eric Lauga. Hydrodynamic attraction of swimming microorganisms by surfaces. Physical Review Letters, 101(3), jul 2008.

[6] Frédéric Bernardin. Multivalued stochastic differential equations: Convergence of a numerical scheme. Set-Valued Analysis, 11(4):393–415, Dec 2003.

[7] Silvio Bianchi, Filippo Saglimbeni, and Roberto Di Leonardo. Holographic imaging reveals the mechanism of wall entrapment in swimming bacteria. Physical Review X, 7(1), jan 2017.

[8] Barath Ezhilan, Roberto Alonso-Matilla, and David Saintillan. On the distribution and swim pressure of run-and-tumble particles in confinement. Journal of Fluid Mechanics, 781, sep 2015.

[9] Guanglai Li, James Bensson, Liana Nisimova, Daniel Munger, Panrapee Mahautmr, Jay X. Tang, Martin R. Maxey, and Yves V. Brun. Accumulation of swimming bacteria near a solid surface. Physical Review E, 84(4), oct 2011.

[10] Guanglai Li and Jay X. Tang. Accumulation of microswimmers near a surface mediated by collision and rotational brownian motion. Physical Review Letters, 103(7), aug 2009.

[11] L. Mertz, G. Stadler, and J. Wylie. A backward Kolmogorov equation approach to compute means, moments and correlations of non-smooth stochastic dynamical systems. ArXiv e-prints, April 2017.

[12] Benoît Perthame. Transport Equations in Biology (Frontiers in Mathematics). Birkhäuser, 2006.

[13] Roger Pettersson. Projection scheme for stochastic differential equations with convex constraints. Stochastic Processes and their Applications, 88(1):125 – 134, 2000.

[14] A. J. Reynolds and Rothschild. The stirring of the medium by bull spermatozoa. Proceedings of the Royal Society of London B: Biological Sciences, 157(969):461–472, 1963.

[15] A. V. Skorokhod. Stochastic equations for diffusion processes in a bounded region. Theory of Probability & Its Applications, 6(3):264–274, 1961.